Abstract

Ventricular assist devices (VADs) are a life-saving form of mechanical circulatory support in heart failure patients. However, VADs have not yet reached their full potential due to the associated side effects (thrombosis, bleeding, infection) related to the activation and damage of blood cells and proteins caused by mechanical stress and foreign materials. Studies of the effects of VADs on leukocytes are limited, yet leukocyte activation and damage including microparticle generation can influence both thrombosis and infection rates. Therefore, the aim was to develop a multicolour flow cytometry assessment of leukocyte microparticles (LMPs) using ovine blood and the CentriMag VAD as a model for shear stress. Ovine blood was pumped for 6 hours in the CentriMag and regular samples analysed for haemolysis, complete blood counts and leukocyte microparticles by flow cytometry during three different pump operating conditions (*low flow*, *standard*, *high speed*). The *high speed* condition caused significant increases in plasma-free haemoglobin; decreases in total leukocytes, granulocytes, monocytes and platelets; increases in $CD45^{+}$ LMPs as well as two novel LMP populations: $CD11b^{bright}$/HLA-DR^{-} and $CD11b^{dull}$/HLA-DR^{+}, both of which were $CD14^{-}$/$CD21^{-}$. $CD11b^{bright}$/HLA-DR^{-} LMPs appeared to respond to an increase in shear magnitude whereas the $CD11b^{dull}$/HLA-DR^{+} LMPs significantly increased in all pumping conditions. We propose that these two populations are released from granulocytes and T cells, respectively, but further research is needed to better characterise these two populations.

Key words:

Flow cytometry, ovine, leukocyte, microparticle, shear stress, ventricular assist, CD11b, HLA-DR, CentriMag

Introduction

Ventricular assist devices (VADs) are a life-saving form of mechanical circulatory support in refractory advanced heart failure patients, either as bridge to heart transplant or as destination therapy [1, 2]. However, VADs have not yet reached their full potential due to the associated side effects (stroke, bleeding, infection, and thrombosis) [3], related to the activation and damage to blood cells and proteins caused by mechanical stress and foreign materials.

Studies of the effects of VADs on leukocytes are limited, yet leukocyte activation and damage can potentially influence both thrombosis and infection rates [4]. Clinical data demonstrate that VADs can cause an overall decrease in leukocyte counts [5], supported by *in vitro* studies using bovine blood, which show a device-specific decrease in viable leukocytes [6]. Activation of granulocytes [5] and $CD4^+$ T cell apoptosis [7, 8], initiated by CD40-ligand (CD40L) induction [9, 10], have also been observed in VAD-patients. Studies on allosensitisation have shown that VAD-patients have hyperreactive B cells and increased levels of alloantibodies, probably caused by stimulation by activated T cells as evidenced by increased levels of soluble CD40L [10, 11]. Finally, microparticle (MPs) formation has been demonstrated *in vitro* [12, 13], and clinically [14-17], suggesting a use for them as predictive markers of adverse events [15, 17]. MPs are membrane vesicles released from many different cell types, through activation or apoptosis, with pro-inflammatory, pro-thrombotic, vasoconstrictive, and angiogenic effects [18-21]. Based on these effects it is evident that MPs can play a role in VAD-related thrombosis. Since MPs are mediators of cellular cross-talk [22], and MP levels are increased in patients with sepsis [23, 24] and parasitic infections [25], it is likely that MPs are involved in VAD-related infections. Since different cell types can release MPs, using lineage markers is important to determine the origin of the cell type. CD45 has been used to demonstrate leukocyte MPs (LMPs) in VADs *in vitro* [12, 13], and

CD11b or CD45 have been used to demonstrate LMPs in VAD-patient samples [14, 16]. Unfortunately, the studies linking microparticles to VAD-complications did not employ lineage markers [15, 17], so it remains unknown which parent cell type(s) are predictive of VAD-complications and there is a need for further studies to better identify MP cellular provenance and quantitative functional capacity before and after LVAD implantation [26].

The above mentioned examples demonstrate that VADs have an impact on leukocytes. However, the results are disarrayed by different device designs tested (including HeartMate XVE, HeartMate II, PVAD, HVAD, CentriMag, VentrAssist, Circulite, and RotaFlow), and a lack of lineage markers for leukocytes in the large animals used for pre-clinical studies, typically cows and sheep. This limits the ability to glean cell type specific effects during early *in vitro* and later *in vivo* testing.

The ovine model is used commonly for *in vivo* testing of VADs [27-32], but there is a need for standardised *in vitro* methods to rapidly assess leukocyte damage of new device designs to enable the development of VADs with fewer side effects. Therefore, the purpose of this study was to: 1) develop an *in vitro* method for studying leukocyte microparticles in ovine blood that can be used by device developers during the screening of new device designs, and 2) identify the parent cell type and activation status of the leukocyte microparticles formed in the CentriMag pump during *in vitro* testing.

Methods

Blood Preparation

Ovine blood was collected by venepuncture using an 11 G x 44 mm stainless steel needle from live sheep (sourced from Ig-Innovations Ltd, Llandysul, UK, project licence (PPL) number 40/3538). The blood was collected into 14% Citrate Phosphate Dextrose Adenine anticoagulant solution and antibiotics / antimycotics. Ovine venepuncture blood was used as opposed to abattoir blood previously [33] due to the poor quality of the blood as a result of the release of mechanically fragile young erythrocytes from the spleen [34].

Automated Haematology Analysis

Complete blood counts were measured using the veterinary analyser Abacus Jr Vet 5 (Diatron, Budapest, Hungary).

Device Operation and Specifications

The extracorporeal ventricular assist device CentriMag® CP (Abbott Vascular, Santa Clara, CA, USA) was tested using an *in vitro* testing circuit under constant haemodynamic conditions using three different operating conditions: herein called *standard*, *low flow*, and *high speed*. The *standard* operating conditions have been described in detail elsewhere [13] and followed the American society for testing and materials (ASTM) standards [35, 36]. Briefly, the flow rate was 5 ± 0.25 L/min, the differential pressure across the pump was adjusted using a custom-made clamp to 100 ± 3 mmHg, and the speed was 2,200 rpm. The *low flow* condition differed by using a flow rate of 1 ± 0.25 L/min, and the *high speed* condition differed by using a speed of 3,300 rpm.

Haemolysis

One ml blood samples were collected hourly and centrifuged at 4700 x g for 7 min. The plasma supernatant (100 µl) was transferred from each aliquot into a deep well 96-well plate (StarLabs, Milton Keynes, UK) and diluted with 1 ml 0.1% Na_2CO_3 solution (Sigma-Aldrich, Poole, UK). 170 µl diluted plasma was transferred into a 96-well flat bottom plate (ELISA plate, Greiner Bio-One, Stonehouse, UK) and the absorbance was measured at three wavelengths: 380, 415, and 450 nm (POLARstar Omega, BMG LABTECH Ltd., Aylesbury, UK). The plasma-free haemoglobin (pfHb) was calculated by the Harboe direct spectrophotometric method (Eq. (1)) as described [37]. (1)

$$(1)\ pfHb\ \left(\frac{g}{L}\right) = (167.2\ x\ A_{415} - 83.6\ x\ A_{450} - 83.6\ x\ A_{380}) \times \left(\frac{1}{1000}\right) x\ (1/\frac{Vol_{plas}}{Vol_{Na_2C}} \quad (2)$$

The normalized index of haemolysis (*NIH*) was calculated as described by (2) [36].

$$NIH\ (\frac{g}{100\ L}) = \Delta pfHb \times V \times \frac{100 - Ht}{100} \times \frac{100}{Q \times T}$$

Where:
NIH = normalized index of haemolysis (g/100L)
ΔpfHb = increase of plasma free haemoglobin concentration (g/L) over the sampling time interval
V = Circuit volume (L)
Q = Flow rate (L/min)
Ht = Haematocrit (%)
T = Sampling time (min)

Flow Cytometry

Sample Treatment and Reagents

Leukocyte Microparticles

Blood samples from time points 5, 120, 240, and 360 min were stained with CD45-PE (Thermo Fisher Scientific, Gloucester, UK) for 30 min on ice in the dark. The red blood cells were lysed by adding EasyLyse (1:20 with dH_2O, DAKO, Alere, Cheshire, UK), followed by vortexing and 15 min incubation at room temperature in the dark. Necrotic cells were stained with 7AAD solution (eBioscience, Hatfield, Ireland, UK) at room temperature in the dark for 15 min before acquisition. As a positive control for 7AAD staining of dead cells, 1 ml baseline blood was treated with Staurosporin solution (Sigma-Aldrich) at room temperature for at least 4 h prior to staining with CD45-PE and 7AAD. Untreated blood was single-stained with CD45-PE and was used to set the 7AAD-gate.

Leukocyte Activation

Blood samples from time points 5, 120, 240, and 360 min were stained with a panel including activation and lineage markers. The antibodies were used according to manufacturer's instructions: anti-CD11b-FITC (AbD Serotec, Oxford, UK), anti-CD21-PE (AbD Serotec) [38], anti-CD14-BDV500 (BD Bioscience, Oxford, UK), and anti-HLA-DR-PE-Cy7 (eBioscience). CD11b and HLA-DR were chosen based on their clinical relevance in monitoring of systemic inflammation response caused by cardiopulmonary bypass pumps (CPB). CD11b is part of the β2 integrin CR3 (complement receptor 3; αMβ2; Mac-1; CD11b/CD18) [39] and is expressed on neutrophils, monocytes, and NK cells [40]. CD11b is upregulated on activated neutrophils in CPB patient blood [41] and has been suggested as a predictive marker of acute renal injury in this patient group [42]. Increased HLA-DR expression is a sign of T cell activation, and HLA-DR is upregulated on T cells in patients

suffering from dilated cardiomyopathy [43]. On the contrary, HLA-DR expression on lymphocytes is decreased by CPB [41], so it is unclear how T cells might respond to the VAD. HLA-DR is also decreased on monocytes after CPB [44-46]. CD14 was first identified on the surface of monocytes and macrophages [47]. Although recent evidence shows its expression is not restricted to myeloid cells [48], it was chosen because it is conventionally used as a monocyte marker for flow cytometry [49]. CD21 was chosen because of its use as an ovine B cell marker, targeting a subset of ovine B cells [50, 51]. Samples were vortexed and incubated on ice for 30min in the dark. EasyLyse (1:20 with dH_2O) was added to the samples which were immediately vortexed and incubated for 15 min at room temperature in the dark to lyse the red blood cells. Antibody-capture (AbC) beads (Thermo Fisher Scientific) were single-stained and used as compensation controls. Fluorescence-minus-one (FMO) controls were used for all antibodies by staining samples subjected to medium insult (240 min CentriMag time point). Isotype controls, isotype-FITC (AbD Serotec, Oxford, UK) and isotype-PE-Cy7 (eBioscience) were used for the activation markers also using the medium insult samples.

Data Acquisition

Samples were acquired with a Navios flow cytometer equipped with three lasers (violet: 405 nm, blue: 488 nm, red: 638 nm), the standard filter configuration, and with *Navios Cytometry List Mode Data Acquisition and Data Analysis Software Navios Cytometer 1.2* software (Beckman Coulter, High Wycombe, UK). Forward scatter (FSC), side scatter (SSC), and fluorescent voltages were set using unstained samples and all samples were recorded for 60 sec. Stained AbC bead samples were acquired using a gate around the beads and capturing 10,000 events.

Quality Control Measures

The instrument was maintained using daily cleaning procedures recommended by the manufacturer throughout the study period. The quality control used the Flow-Check and Flow-Set Pro Fluorospheres (Beckman Coulter) and the protocols used were set-up by the manufacturer's technical support engineers.

Data Analysis

All data were exported and analysed using automatic compensation in Kaluza 1.5a (Beckman Coulter) using the data from the AbC bead samples. Data were displayed on FSC and SSC logarithmic axes and fluorescence displayed on bi-exponential axes [52].

Leukocytes were gated and displayed on a contour density dot plot with 7AAD against CD45-PE. The healthy cell gate was set using the Staurosporin-treated control to just outside the main contour of the healthy 7AAD-negative population (Supplementary Figure 1). Any events to the right of this border were considered 7AAD-positive necrotic leukocytes. Fragmented white blood cells (LMPs) still display CD45 but no longer contain DNA and because of their reduced size and complexity, and therefore lower side scatter, end up below the healthy leukocytes on an SSC axes in the gate designated MP.

The gating strategy was drawn using the baseline samples and comparing the pattern differences to the pumped samples which were obvious (see for example Figure 3). FMOs for all antibodies, and isotype controls for the activation markers CD11b and HLA-DR, were prepared but did not prove useful in this lyse no wash protocol. Isotype controls were useful for setting the gates for the cells but not for the microparticles (Supplementary Figure 2).

Statistical Methods

Averages and standard deviations were calculated for all parameters and time points. Leukocyte microparticles and complete blood counts were divided by the static control at time point 5 minutes to evaluate the relative increase or decrease caused by duration of pumping whilst minimising donor-to-donor variability. For haemolysis, the background levels observed at 5 minutes were subtracted from all other measurements. The dataset consisted of repeated measurements of blood samples across three pumping conditions and 4 or 7 time points (7 for haemolysis, 4 for the other assays). Linear mixed models were used to analyse the dataset. The reason we used a LMM was because the observations were in the form of repeated measures, which introduced possible hierarchical effects. By using LMM we were able to allow for these. In particular, we included individual level random effects (intercept and rate of change) in addition to the fixed effects. Differences between the groups at time point 360 min were assessed with the Kruskal-Wallis test and post-hoc pairwise comparisons. All statistical data analysis was performed in SPSS version 22 (SPSS, Inc., Chicago, Illinois, US).

Results

Ovine blood was run through a 2 m loop, powered by a CentriMag under 3 different testing conditions (Table 1).

Haematology

There was no significant difference in the red blood cell count for either the static or the pumped samples (Fig 1A). The white cells decreased significantly in the *high speed* condition ($p = 0.001$). Both the *standard* and the *high speed* caused a significant decrease in the granulocyte count compared to the static control ($p = 0.006$ and $p < 0.001$, respectively) but only the *high speed* condition caused a decrease in the monocyte count versus the static control ($p = 0.003$). There were no changes to the lymphocyte count. The platelets decreased significantly in both the *low flow* and *high speed* condition compared to the static ($p = 0.005$ and $p = 0.008$, respectively).

Haemolysis

The pfHb levels for all testing conditions increased over time as expected (Fig 1B). The lowest pfHb levels were observed in the tests run at *low flow*, with pfHb measured at 0.7 ± 0.6 mg/dL at 6 hours. The highest levels of pfHb were observed in the tests run at *high speed*; pfHb measured at 7.3 ± 5.0 mg/dL at 6 hours, which was significantly different compared to the static control ($p < 0.001$).

Leukocyte microparticles

All pumping conditions caused a significant increase in $CD45^+$ LMPs compared to the static control (*low flow:* $p = 0.005$, *standard*: $p = 0.004$, *high speed*: $p < 0.001$; Fig 1C). An example of the flow cytometry data from the *high speed* condition over time is shown (Fig 2). The antibodies were tested on baseline blood to confirm that they could detect the target

parent cells (Supplementary Figure 3). CD14-BDV500 detected granulocytes (high SSC/CD14^{dull}), and monocytes (medium-high SSC/CD14^{+}). CD21-PE stained a B cell subset (medium SSC/CD21^{+}). CD11b-FITC mainly stained granulocytes, monocytes, and a subset of lymphocytes. HLA-DR-PE-Cy7 targeted monocytes and a subset of lymphocytes. Gated medium-high SSC/CD14^{+} monocytes were CD11b^{+} and about 60% also expressed HLA-DR. Of the CD21^{+} B cells, around 50% were HLA-DR^{+}/CD11b^{-}, and approximately 40% were double positive.

Characterisation of LMPs

LMPs generated during pump testing expressed CD11b and/or HLA-DR (Figure 3). Three subpopulations could be identified: CD11b^{bright}HLA-DR^{+}, CD11b^{dull}HLA-DR^{+}, and CD11b^{bright}HLA-DR^{-} (Fig 4A). All three populations were negative for both CD14 and CD21 (Fig 4B), so are unlikely to be derived from monocytes or the CD21^{+} B cell subset. On specifically seeking CD14^{+} or CD21^{+} LMPs there were none detectable (Supplementary Figure 4). Since HLA-DR expression was restricted to the monocyte/lymphocyte side scatter area (Fig 3C), the parental lineage is unlikely to be granulocytes and we propose T cells or CD21^{-} B cells as the most likely parental lineages for the CD11b^{dull}HLA-DR^{+} LMPs. The parental lineage for the CD11b^{bright}HLA-DR^{-} population is most likely granulocytes, due to their high CD11b expression (Fig 3B) and lack of HLA-DR (Fig 3C). The small CD11b^{bright}HLA-DR^{-} population could be a further activated subset from either of the granulocyte or lymphocyte MP populations, as both activated T cells can increase their CD11b expression [53], and activated neutrophils can increase their HLA-DR expression [54].

Influence of Pumping Condition on Activated LMP Production

The *standard* and the *high speed* condition caused a significant increase in the $CD11b^{bright}HLA\text{-}DR^{-}$ LMPs versus the static control ($p = 0.027$ and $p < 0.001$, respectively) (Figure 4C). The *high speed* also caused a significant increase for the $CD11b^{bright}HLA\text{-}DR^{+}$ LMPs compared to the static control ($p < 0.001$) (Figure 4D). The $CD11b^{dull}HLA\text{-}DR^{+}$ LMPs significantly increased during all pumping conditions compared to the static control ($p < 0.001$) (Figure 4E). Finally, at 360 min, the *high speed* condition caused significantly more $CD11b^{bright}HLA\text{-}DR^{-}$ LMPs compared to $CD11b^{dull}HLA\text{-}DR^{+}$ LMPs ($p = 0.002$).

Discussion

To the best of our knowledge this is the first study to describe a four colour flow cytometry panel for ovine leukocytes; previous studies have used single or two-colour approaches [55-58]. It is also the first time LMPs displaying activation markers have been shown to be generated during *in vitro* VAD testing, and the first time LMPs have been demonstrated *in vitro* using ovine blood. This study also represents the first ovine blood damage profile for the CentriMag operated under standard conditions (as defined by ASTM [35, 36]). The panel described herein can be used to detect differences in LMP generation due to shear stress as demonstrated by pumping whole blood in the CentriMag, a suggested benchmark for *in vitro* VAD-testing [13], at different operating conditions. The antibodies used were chosen on two criteria: 1) directly conjugated to fluorochromes for replicability and uptake by other users, and 2) cross reactivity to ovine, bovine, and human blood cells, to yield a translational research tool suitable for device developers using animals in the pre-clinical phase and then progressing to clinical studies.

Similarly to our previously published bovine CentriMag blood damage profile [13], the *standard* condition did not cause any significant differences to ovine total red cell, white cell, or platelet counts. However, now we also studied the leukocyte subsets, and show that the *standard* condition caused a significant reduction in the granulocyte count. Perhaps because the lymphocytes are the most prevalent white blood cell type in bovine and ovine blood [59], and lymphocyte counts remained constant in this ovine blood study, they mask the decreasing granulocytes levels when only the total white blood cell count is measured.

The *high speed* condition caused a reduction in both granulocyte and monocyte counts, but lymphocytes remained constant. This reflects either the resilience of lymphocytes or their abundance in the ovine circulation [59]. Consideration of lymphocyte subsets and/or a higher

resolution method such as absolute counting using flow cytometry [33] might be required to assess any decrease in lymphocyte cell numbers. Both the *low flow* and the *high speed* conditions significantly decreased platelet counts. Platelet activation is caused by both an increase in residence time (as in the *low flow* condition)[60], and by high shear stress [61, 62] which could lead to lysis and/or aggregation and the observed reduction in numbers. Interestingly, our previous study of bovine blood using the extracorporeal RotaFlow and the intracorporeal VentrAssist pumps observed an increase in platelet numbers [12]. This increase was hypothesised to be due to leukocyte microparticles being falsely detected as platelets by the haematology analyser due to the concomitant decrease in leukocytes and increase in $CD45^+$ LMPs [12]. Although the *high speed* condition in this current study caused a reduction in leukocytes and an increase in $CD45^+$ LMPs, there was no increase in platelets. This could be due to different haematology analysers being used in the two studies (CELL-DYN Ruby versus Abacus Jr Vet 5).

The haemolysis data showed evidence of increased resilience of ovine venepuncture versus bovine abattoir erythrocytes to the effects of shear. Levels of pfHb obtained with ovine blood were one quarter of those obtained in bovine blood after 360 minutes pumping in the CentriMag at the *standard* condition (2.5 ± 1.0 versus 10 ± 1.5 mg/dL), with mgNIH roughly one third in ovine compared to bovine blood (0.38 ± 0.15 compared to 1.10 ± 0.5 mg/100L) [13]. In our previous multispecies comparison study in which we evaluated the response to shear caused by a rheometer, we also observed greater haemolysis in bovine abattoir compared to ovine venepuncture blood at high shear (75 versus 50 mg/dL at 8000 s^{-1}, respectively), although this difference was not statistically significant [34].

The *standard* condition in this study caused a significant increase in ovine $CD45^+$ LMPs, as previously observed in bovine blood [13]. In addition, the $CD45^+$ LMPs significantly

increased in the *low flow* and the *high speed* conditions as well. We have confirmed the LMP identity in a previous study [12], where we showed that: $CD45^+$ LMPs were a fraction of the size compared to $CD45^+$ leukocytes using imaging cytometry; we showed microparticles, morphologically different from platelets, in association with leukocytes using scanning electron microscopy; and we showed that, when using bovine activated platelet marker GC5A, the FSC/SSC region co-habited by microparticles and platelets consists of 3 separate populations: $CD45^+$ LMPs, activated $GC5A^-$ platelets, and resting $GC5A^+$ platelets.

In this study, three novel ovine LMP populations were identified: $CD11b^{bright}HLA\text{-}DR^+$, $CD11b^{dull}HLA\text{-}DR^+$, and $CD11b^{bright}HLA\text{-}DR^-$. These were all negative for CD14 and CD21, suggesting they are not derived from monocytes or the $CD21^+$ B cell subset. However, it is possible that as there are relatively few monocytes in ovine blood [59], monocyte-derived LMPs might simply be relatively rare and undetectable. The remaining major cell types are neutrophils, T cells, and $CD21^-$ B cells. Neutrophils express CD11b, and have been shown to produce $CD11b^+$ MPs when activated *in vitro* [63-65]. Considering that the granulocyte cell count (Fig 1) and the $CD11b^{bright}HLA\text{-}DR^-$ frequency (Fig 4C) were both the most affected by the *high speed* condition, this further supports that the $CD11b^{bright}HLA\text{-}DR^-$ MPs are of neutrophil origin. Excluding granulocytes ($CD11b^{bright}$), and monocytes ($CD14^+$), T cells, or $CD21^-$ B cells are the most likely parent of the $CD11b^{dull}HLA\text{-}DR^+$ MPs. That granulocytes and T cells would be the cell types most affected in the VAD *in vitro*, is supported by clinical evidence showing the activation of both granulocytes and T cells in VAD-patients [5, 7, 8].

This study shed light on two important aspects of leukocyte MPs in relation to VADs. Firstly, it showed that $CD11b^+$ MPs are generated in VADs, which could have implications for pump thrombosis. Low levels of $CD11b^+$ LMPs are a risk factor in patients suffering non-ST elevated acute coronary syndrome, as low levels are associated with a higher number of

occluded arteries, higher number of >50% stenosis, higher number of stenosed arteries, and higher frequency of recurring cardiovascular events, [66]. The decline in $CD11b^{+}$ LMPs is suggestive of their consumption in the occlusions, since $CD11b^{+}$ levels negatively correlate with thrombus weight in a mouse model [19]. The mechanism is likely to be through $\alpha_M\beta_2$ interaction with resting platelets, causing them to become activated [65].

Secondly, it showed that different LMP subtypes respond differently to changes in operating conditions. The $CD11b^{dull}HLA\text{-}DR^{+}$ LMPs were sensitive to pumping and significantly increased regardless of the operating conditions. However, they did not respond to a further increase in speed. In contrast, the levels of $CD11b^{bright}HLA\text{-}DR^{-}$ LMPs were not significantly different from the static control in any other condition than the *high speed* so are seemingly more affected by increasing speed than the $CD11b^{dull}HLA\text{-}DR^{+}$ LMPs. Hence, the $CD11b^{dull}HLA\text{-}DR^{+}$ LMPs show potential as a positive control for pumping versus static samples, and the $CD11b^{bright}HLA\text{-}DR^{-}$ LMPs may be able to differentiate between the effects of pump designs on LPM generation if the pumps differ in shear stress. The different responses to the operating conditions further supports that these LMPs are of different cellular origins. *In vitro* studies of human leukocytes under shear stress have revealed that the fluid shear response is not uniform among all cells. At low shear stress levels (0.2 dyn/cm^2 for 5 min) about 33% of leukocytes respond with pseudopodia projection [67]. These first responders could be lymphocytes since they make up 17-48 % of the human leukocyte count, whereas neutrophils make up 40-75% [68]. The number of human leukocytes responding to shear stress increases with each 1 dyn/cm^2 [67]. This could be the neutrophils as they have been described to display a dose-response relationship with both shear magnitude and time *in vitro* using a cone-and-plate viscometer, with L-selectin shedding as the measure [69]. Lastly,

the migration of human T cells and neutrophils *in vitro* also differs with T cells migrating against the fluid flow and neutrophils migrating with it [70].

Study Limitations

One study limitation was to find antibodies that target ovine blood cells. For example, there is no ovine platelet lineage marker that is not affected by activation which is why platelet MPs were not studied. This also means we cannot analyse the potential platelet contamination within the leukocyte MP population. However, a confirmatory experiment using human blood double-stained with platelet and leukocyte lineage markers CD41 and CD45, respectively, pumped using the 'high speed' protocol, showed that within the $CD45^{+}$ MP population, there is a 10% contamination of double-positive platelet aggregates (Supplementary Figure 5). Thus, if the assay is used with human blood, an initial platelet-discrimination gate can be set to exclude platelet-MP aggregates from further analysis steps, if desired.

In addition, there is no directly conjugated anti-ovine granulocyte antibody available to confirm that the $CD11b^{bright}$ MPs were of neutrophil origin. For future studies, in-house conjugation of the granulocyte-monocyte targeting antibody clone, DH59B [56], could be used in combination with anti-CD14 to distinguish the granulocyte ($DH59B^{+}CD14^{+}$) and monocyte ($DH59^{bright}CD14^{bright}$) MPs.

Although there is a vast amount of literature describing that MPs can be identified using lineage markers [21, 71-73], a couple of studies have described contradictory results. Monocyte and lymphocyte MPs, in particular B cell MPs, have been described to lack lineage markers [74, 75]. In addition, human malignant B cell MPs, but not T cell MPs, have been described to express HLA-DR [75], hence the $CD11b^{dull}$HLA-DR^{+} LMPs could be B cell MPs that are not expressing CD21; this remains to be proven.

The method described herein was developed as a whole blood wash-no-lyse protocol in order to fit around the routine haemolysis procedures of a device testing lab. As per the ASTM

standard, haemolysis testing should be carried out on fresh blood for a total of 6 hours [36]. In practice, this means that any samples collected from such a test will be available in the evening. We deemed an MP isolation method including several centrifugation steps would be too time-consuming for it to be practical to do in addition to a haemolysis test for most device developers. Thus, we opted for a rapid whole blood staining protocol to make it user friendly.

Lastly, conventional flow cytometric methods use standardisation beads to define the initial FSC/SSC scatter gate for further MP analysis. Although we did not use such beads, the method is fully compatible with beads as exemplified by a subsequent acquisition of Megamix beads using the same acquisition protocol. When displaying the MP population in a Megamix gate created around the FSC/SSC of beads 900 nm and smaller, 92% of the $CD45^+$ MP population was within the gate (Supplementary Figure 6). Thus, an additional Megamix bead gate could be introduced, if desired.

Conclusion

This first report of the blood damage profile of ovine blood exposed to the CentriMag pump shows that ovine venepuncture blood may potentially be more resilient than bovine abattoir blood to shear stress. This is supported by our previous multispecies rheometry study [34]. As expected, the *high speed* condition was the most detrimental regarding all parameters. This condition caused a significant decrease in total leukocytes, granulocytes, monocytes and platelets; an increase in pfHb; and an increase in $CD45^{+}$ LMPs, and, using a 4-colour panel for ovine leukocytes for the first time, an increase in three novel LMP populations: $CD11b^{bright}HLA\text{-}DR^{+}$, $CD11b^{dull}HLA\text{-}DR^{+}$, and $CD11b^{bright}HLA\text{-}DR^{-}$.

We propose that this multicolour panel can be used by device developers to test and develop VADs with better blood handling capacity for reduced side effects. Our next step is to repeat this study in bovine blood using several device types and to expand the flow cytometry panel used to include granulocyte and T cell markers based on the results presented herein. This will confirm if the panel is useful for monitoring LMP formation during *in vitro* testing in bovine blood and promote its further adoption by the industry. It will also enable us to identify the parental lineage of LMPs and undertake pump comparison testing. This study also highlights the need to better understand the formation and functional effects of circulating LMPs in humans implanted with VADs.

Acknowledgments

[removed due to blinding – see Cover Letter]

Conflicts of Interest

[removed due to blinding – see Cover Letter]

References

1. Patel, S., et al., *Left ventricular assist device: a bridge to transplant or destination therapy?* Postgraduate medical journal, 2016: p. postgradmedj-2015-133718.
2. Birks, E.J., et al., *The role of bridge to transplantation: should LVAD patients be transplanted?* Current opinion in cardiology, 2004. **19**(2): p. 148-153.
3. Krabatsch, T., et al., *Heartmate 3 fully magnetically levitated left ventricular assist device for the treatment of advanced heart failure –1 year results from the Ce mark trial.* Journal of Cardiothoracic Surgery, 2017. **12**(1): p. 23.
4. Itescu, S., et al., *Immunobiology of left ventricular assist devices.* Progress in cardiovascular diseases, 2000. **43**(1): p. 67-80.
5. Woolley, J.R., et al., *Temporal Leukocyte Numbers and Granulocyte Activation in Pulsatile and Rotary Ventricular Assist Device Patients.* Artificial Organs, 2013.
6. Takami, Y., et al., *Mechanical white blood cell damage in rotary blood pumps.* Artif Organs, 1997. **21**(2): p. 138-42.
7. Ankersmit, H.J., et al., *Quantitative changes in T-cell populations after left ventricular assist device implantation: relationship to T-cell apoptosis and soluble CD95.* Circulation, 1999. **100**(19 Suppl): p. II211-5.
8. Ankersmit, H.J., et al., *Activation-induced T-cell death and immune dysfunction after implantation of left-ventricular assist device.* Lancet, 1999. **354**(9178): p. 550-5.
9. Schuster, M., et al., *Induction of CD40 ligand expression in human T cells by biomaterials derived from left ventricular assist device surface.* Transplant Proc, 2001. **33**(1-2): p. 1960-1.
10. Schuster, M., et al., *B-cell activation and allosensitization after left ventricular assist device implantation is due to T-cell activation and CD40 ligand expression.* Hum Immunol, 2002. **63**(3): p. 211-20.
11. Velez, M. and M.R. Johnson, *Management of allosensitized cardiac transplant candidates.* Transplantation reviews, 2009. **23**(4): p. 235-247.
12. Chan, C.H., et al., *The evaluation of leukocytes in response to the in vitro testing of ventricular assist devices.* Artificial Organs, 2013. **37**(9): p. 793-801.
13. Chan, C.H., et al., *The CentriMag centrifugal blood pump as a benchmark for in vitro testing of hemocompatibility in implantable ventricular assist devices.* Artif Organs, 2015. **39**(2): p. 93-101.
14. Diehl, P., et al., *Enhanced microparticles in ventricular assist device patients predict platelet, leukocyte and endothelial cell activation.* Interact Cardiovasc Thorac Surg, 2010. **11**(2): p. 133-7.
15. Nascimbene, A., et al., *Association between cell-derived microparticles and adverse events in patients with nonpulsatile left ventricular assist devices.* J Heart Lung Transplant, 2014. **33**(5): p. 470-7.
16. Sansone, R., et al., *Macrovascular and microvascular function after implantation of left ventricular assist devices in end-stage heart failure: Role of microparticles.* J Heart Lung Transplant, 2015. **34**(7): p. 921-32.
17. McClane, N., et al., *Identification & Characterization of Novel Hemostatic Biomarkers of Adverse Clinical Events in Patients with Continuous Flow Left Ventricular Assist Device Implants.* The FASEB Journal, 2017. **31**(1 Supplement): p. 978.4-978.4.
18. VanWijk, M.J., et al., *Microparticles in cardiovascular diseases.* Cardiovascular Research, 2003. **59**(2): p. 277-287.

19. Ramacciotti, E., et al., *Leukocyte- and platelet-derived microparticles correlate with thrombus weight and tissue factor activity in an experimental mouse model of venous thrombosis.* Thromb Haemost, 2009. **101**(4): p. 748-54.
20. Owens, A.P. and N. Mackman, *Microparticles in hemostasis and thrombosis.* Circulation research, 2011. **108**(10): p. 1284-1297.
21. Angelillo-Scherrer, A., *Leukocyte-derived microparticles in vascular homeostasis.* Circulation Research, 2012. **110**(2): p. 356-369.
22. Distler, J.H., et al., *Microparticles as mediators of cellular cross-talk in inflammatory disease.* Autoimmunity, 2006. **39**(8): p. 683-690.
23. Soriano, A.O., et al., *Levels of endothelial and platelet microparticles and their interactions with leukocytes negatively correlate with organ dysfunction and predict mortality in severe sepsis.* Critical care medicine, 2005. **33**(11): p. 2540-2546.
24. Fujimi, S., et al., *Activated Polymorphonuclear Leukocytes Enhance Production of Leukocyte Microparticles with Increased Adhesion Molecules in Patients with Sepsis.* Journal of Trauma and Acute Care Surgery, 2002. **52**(3): p. 443-448.
25. Campos, F.M., et al., *Augmented plasma microparticles during acute Plasmodium vivax infection.* Malaria journal, 2010. **9**(1): p. 327.
26. Shah, K.B. and M.C. Kontos, *Microparticles and left ventricular assist device complications: a causal association?* J Heart Lung Transplant, 2014. **33**(5): p. 468-9.
27. Tuzun, E., et al., *In vivo performance evaluation of the innovamedica pneumatic ventricular assist device.* Asaio j, 2012. **58**(2): p. 98-102.
28. Tuzun, E., et al., *In vivo evaluation of investigation the HeartWare centrifugal ventricular assist device.* Texas Heart Institute Journal, 2007. **34**(4): p. 406-411.
29. Zhang, Y., et al., *In vivo experimental testing of the FW axial blood pump for left ventricular support in Fu Wai Hospital.* Asaio j, 2009. **55**(1): p. 28-32.
30. Voitl, P., et al., *Coronary hemodynamics and myocardial oxygen consumption during support with rotary blood pumps.* Artif Organs, 2009. **33**(1): p. 77-80.
31. Spurlock, D.J., et al., *Preliminary in vivo testing of a novel pump for short-term extracorporeal life support.* Ann Thorac Surg, 2012. **93**(1): p. 141-6.
32. Wei, X., et al., *Initial experience with a juvenile sheep model for evaluation of the pediatric intracorporeal ventricular assist devices [corrected]*. Asaio j, 2013. **59**(1): p. 75-80.
33. Pieper, I.L., et al., *Quantification methods for human and large animal leukocytes using DNA dyes by flow cytometry.* Cytometry Part A, 2016: p. 565-74.
34. Chan, C. and I.L. Pieper, *Multispecies study - update when published!* 2017.
35. ASTM, *F1830-97: Standard Practice for Selection of Blood for in vitro Evaluation of Blood Pumps*. 2013.
36. ASTM, *F1841-97: Standard Practice for Assessment of Hemolysis in Continous Flow Blood Pumps*. 2013.
37. Han, V., K. Serrano, and D. Devine, *A comparative study of common techniques used to measure haemolysis in stored red cell concentrates.* Vox sanguinis, 2010. **98**(2): p. 116-123.
38. Griebel, P.J., et al., *Cross-reactivity of mAbs to human CD antigens with sheep leukocytes.* Veterinary immunology and immunopathology, 2007. **119**(1): p. 115-122.
39. O'Brien, X.M. and J.S. Reichner, *Neutrophil Integrins and Matrix Ligands and NET Release.* Front Immunol, 2016. **7**: p. 363.
40. Li, Z., *The alphaMbeta2 integrin and its role in neutrophil function.* Cell Res, 1999. **9**(3): p. 171-8.

41. McBride, W., et al., *Cytokine balance and immunosuppressive changes at cardiac surgery: contrasting response between patients and isolated CPB circuits.* British journal of anaesthesia, 1995. **75**(6): p. 724-733.
42. Rinder, C.S., et al., *Neutrophil CD11b upregulation during cardiopulmonary bypass is associated with postoperative renal injury.* The Annals of thoracic surgery, 2003. **75**(3): p. 899-905.
43. Ueno, A., et al., *Increases in circulating T lymphocytes expressing HLA-DR and CD40 ligand in patients with dilated cardiomyophthy.* Heart and vessels, 2007. **22**(5): p. 316-321.
44. Döcke, W.-D., et al., *Monitoring temporary immunodepression by flow cytometric measurement of monocytic HLA-DR expression: a multicenter standardized study.* Clinical chemistry, 2005. **51**(12): p. 2341-2347.
45. Oczenski, W., et al., *HLA-DR as a marker for increased risk for systemic inflammation and septic complications after cardiac surgery.* Intensive care medicine, 2003. **29**(8): p. 1253-1257.
46. Allen, M.L., et al., *Early postoperative monocyte deactivation predicts systemic inflammation and prolonged stay in pediatric cardiac intensive care.* Critical care medicine, 2002. **30**(5): p. 1140-1145.
47. Griffin, J.D., et al., *Expression of myeloid differentiation antigens on normal and malignant myeloid cells.* J Clin Invest, 1981. **68**(4): p. 932-41.
48. Jersmann, H.P., *Time to abandon dogma: CD14 is expressed by non-myeloid lineage cells.* Immunology and cell biology, 2005. **83**(5): p. 462-467.
49. Abeles, D., et al., *CD14, CD16 and HLA-DR reliably identifies human monocytes and their subsets in the context of pathologically reduced HLA-DR expression by CD14hi/CD16neg monocytes: Expansion of CD14hi/CD16pos and contraction of CD14lo/CD16pos monocytes in acute liver failure.* Cytometry Part A, 2012. **81**(10): p. 823-834.
50. Booth, J.S., et al., *Co-stimulation with TLR7/8 and TLR9 agonists induce down-regulation of innate immune responses in sheep blood mononuclear and B cells.* Dev Comp Immunol, 2010. **34**(5): p. 572-8.
51. Edwards, J.C., et al., *PrP(Sc) is associated with B cells in the blood of scrapie-infected sheep.* Virology, 2010. **405**(1): p. 110-9.
52. Tung, J.W., et al., *New approaches to fluorescence compensation and visualization of FACS data.* Clin Immunol, 2004. **110**(3): p. 277-83.
53. Kotsougiani, D., et al., *Activation of T Lymphocytes in Response to Persistent Bacterial Infection: Induction of CD11b and of Toll-Like Receptors on T Cells.* International Journal of Inflammation, 2010. **2010**: p. 10.
54. Reinisch, W., et al., *Donor dependent, interferon-γ induced HLA-DR expression on human neutrophils in vivo.* Clinical & Experimental Immunology, 2003. **133**(3): p. 476-484.
55. Boppana, D.K., et al., *In vivo immunomodulatory effects of ixodid ticks on ovine circulating T-and B-lymphocytes.* Parasite immunology, 2004. **26**(2): p. 83-93.
56. Smith, H.E., R.M. Jacobs, and C. Smith, *Flow cytometric analysis of ovine peripheral blood lymphocytes.* Canadian Journal of Veterinary Research, 1994. **58**(2): p. 152.
57. Albenzio, M., et al., *Immune competence of the mammary gland as affected by somatic cell and pathogenic bacteria in ewes with subclinical mastitis.* J Dairy Sci, 2012. **95**(7): p. 3877-87.

58. Caroprese, M., et al., *Relationship between cortisol response to stress and behavior, immune profile, and production performance of dairy ewes.* Journal of dairy science, 2010. **93**(6): p. 2395-2403.
59. Jones, M.L. and R.W. Allison, *Evaluation of the ruminant complete blood cell count.* Veterinary Clinics of North America: Food Animal Practice, 2007. **23**(3): p. 377-402.
60. Fraser, K., *Mechanical Stress Induced Blood Trauma*, in *Heat transfer and fluid flow in biological processes*, S.M. Becker and A.V. Kuznetsov, Editors. 2015, Elsevier: USA. p. 305-333.
61. Holme, P.A., et al., *Shear-induced platelet activation and platelet microparticle formation at blood flow conditions as in arteries with a severe stenosis.* Arteriosclerosis, thrombosis, and vascular biology, 1997. **17**(4): p. 646-653.
62. Sheriff, J., et al., *High-shear stress sensitizes platelets to subsequent low-shear conditions.* Annals of biomedical engineering, 2010. **38**(4): p. 1442-1450.
63. Gasser, O., et al., *Characterisation and properties of ectosomes released by human polymorphonuclear neutrophils.* Experimental cell research, 2003. **285**(2): p. 243-257.
64. Dalli, J., et al., *Heterogeneity in neutrophil microparticles reveals distinct proteome and functional properties.* Molecular & Cellular Proteomics, 2013. **12**(8): p. 2205-2219.
65. Pluskota, E., et al., *Expression, activation, and function of integrin αMβ2 (Mac-1) on neutrophil-derived microparticles.* Blood, 2008. **112**(6): p. 2327-2335.
66. Faille, D., et al., *CD11b+ leukocyte microparticles are associated with high-risk angiographic lesions and recurrent cardiovascular events in acute coronary syndromes.* Journal of Thrombosis and Haemostasis, 2011. **9**(9): p. 1870-1873.
67. Coughlin, M.F. and G.W. Schmid-Schönbein, *Pseudopod projection and cell spreading of passive leukocytes in response to fluid shear stress.* Biophysical journal, 2004. **87**(3): p. 2035-2042.
68. Bossche, J.V.d., et al., *Reference intervals for a complete blood count determined on different automated haematology analysers: Abx Pentra 120 Retic, Coulter Gen-S, Sysmex SE 9500, Abbott Cell Dyn 4000 and Bayer Advia 120.* Clinical chemistry and laboratory medicine, 2002. **40**(1): p. 69-73.
69. Mitchell, M., K. Lin, and M. King, *Fluid Shear Stress Increases Neutrophil Activation via Platelet-Activating Factor*. Biophys J, 2014. **106**(10): p. 2243-53.
70. Valignat, M.P., et al., *T Lymphocytes Orient against the Direction of Fluid Flow during LFA-1-Mediated Migration.* Biophys J, 2013. **104**(2): p. 322-31.
71. Headland, S.E., et al., *Cutting-edge analysis of extracellular microparticles using ImageStreamX imaging flow cytometry.* Scientific reports, 2014. **4**: p. 5237.
72. Gelderman, M.P. and J. Simak, *Flow cytometric analysis of cell membrane microparticles.* Methods Mol Biol, 2008. **484**: p. 79-93.
73. Simak, J. and M.P. Gelderman, *Cell membrane microparticles in blood and blood products: potentially pathogenic agents and diagnostic markers.* Transfus Med Rev, 2006. **20**(1): p. 1-26.
74. Crompot, E., et al., *Avoiding false positive antigen detection by flow cytometry on blood cell derived microparticles: the importance of an appropriate negative control.* PloS one, 2015. **10**(5): p. e0127209.
75. Miguet, L., et al., *Proteomic analysis of malignant lymphocyte membrane microparticles using double ionization coverage optimization.* Proteomics, 2006. **6**(1): p. 153-171.

Acknowledgments

The authors would like to thank Innovate UK for the Biomedical Catalyst Award (reference: 101462) provided to Calon Cardio-Technology Ltd and Swansea University. The authors would also like to thank Dr Graham Foster for his instrumental role in securing funding for this research.

Conflicts of Interest

Authors Ina Laura Pieper, Sabrina Ali and Abigail Christen are employees of Calon. Gemma Radley is a PhD-student jointly funded by Calon and Swansea University. Authors Owen Bodger and Catherine A. Thornton have no conflicts of interest.

Tables

Table 1. Operating conditions

	Low flow	*Standard*	*High speed*
Speed (rpm)	2200 ± 0	2200 ± 82	3300 ± 0
Flow (L/min)	1.00 ± 0.03	5.03 ± 0.08	4.96 ± 0.06
Pressure (mmHg)	105.29 ± 1.91	82.98 ± 4.59	212.23 ± 19.14
mgNIH at 360 min (mg/100L)	1.05 ± 0.89	0.38 ± 0.15	2.82 ± 2.80
Baseline Hct (%)	30.33 ± 2.57	30.78 ± 1.49	29.25 ± 3.88
Baseline Hb (g/L)	116.27 ± 15.55	116.03 ± 15.05	108.11 ± 12.36
Sample size (n)	4	5	5

Figure Legends

Figure 1. Haematology, Haemolysis, and Leukocyte Microparticles Generated in the Centrimag Under Different Conditions.

Ovine blood was diluted to a haematocrit of 30 ± 2% using PBS, loaded into the CentriMag loop and run at either *low flow*: 2,200 rpm, 1 L/min (n = 3), *standard* conditions: 2,200 rpm, 5 L/min (n = 5), or *high speed*: 3,300 rpm, 5 L/min (n = 5). A 500 mL bag of ovine blood was left in the +37°C water bath as a static control. Blood samples were removed every hour for 6 hours. **A.** Average complete cell counts from blood samples run in triplicate for erythrocytes, leukocytes, platelets, granulocytes, monocytes, and lymphocytes for each time point. **B.** Plasma free haemoglobin. **C.** Number of CD45 positive ($CD45^{+}$) microparticles.

Figure 2. Baseline Blood Characterisation.

Ovine whole blood stained with antibodies targeting CD14, CD21, CD11b, and HLA-DR. **A.** Granulocytes have high side scatter (SSC) and are $CD14^{dull}$. Monocytes (gated) have medium-high SSC and are $CD14^{+}$. **B.** Some B cells have medium SSC and are $CD21^{+}$. **C.** CD11b is mainly expressed by granulocyte and monocytes and a subset of lymphocytes. **D.** HLA-DR expression is restricted to monocytes and a subset of lymphocytes. **E.** Monocytes are $CD11b^{+}$ and around 60% are HLA-DR^{+}. **F.** Of $CD21^{+}$ B cells, about 50% are HLA-DR^{+}/$CD11b^{-}$, and approximately 40% are double positive.

Figure 3. Scatter Profile and MP Formation During *High Speed* Pump Setting.

Ovine whole blood pumped in the CentriMag (CMAG) at high speed (3,300 rpm) for 5, 120, 240, and 360 min and compared to baseline. The blood was stained with antibodies targeting CD14, CD21, CD11b, and HLA-DR. FSC / SSC: there is an initial increase in scatter followed by a rapid decline during pumping. $CD11b^{+}$ and HLA-DR^{+} MPs have low SSC and increase in frequency with pumping time.

Figure 4. LMP populations expressing activation markers.

Ovine whole blood pumped in the CentriMag (CMAG) at high speed (3,300 rpm) for 360 min. The blood was stained with antibodies targeting CD14, CD21, CD11b, and HLA-DR, and MPs expressing CD11b and/or HLA-DR were gated. A Boolean gate named Active MPs was created ($CD11b^{+}$ OR HLA-DR^{+} MPs) and displayed. **A.** Active MPs form three distinct populations when displayed on CD11b versus HLA-DR axes. **B.** The three populations are $CD14^{-}$/$CD21^{-}$, and therefore likely to be generated by granulocytes (CD11b) and T cells or $CD21^{-}$ B cells (HLA-DR) based on the baseline cell surface marker expression (Supplementary Figure 3).

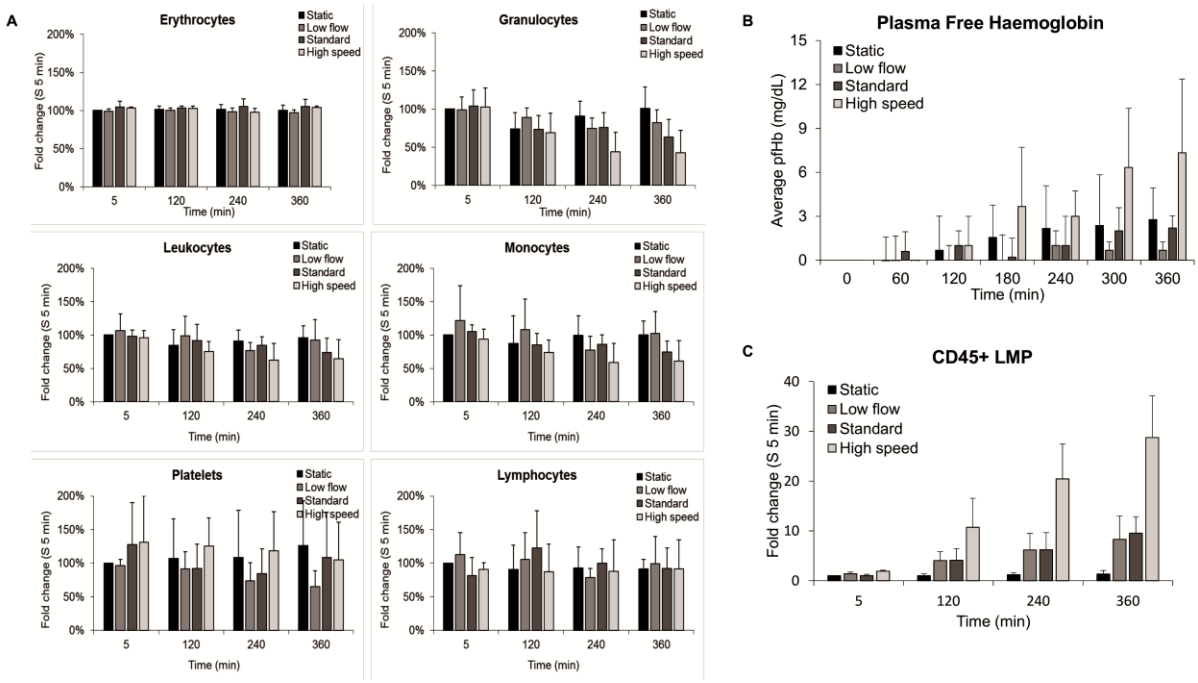
A
Erythrocytes
Granulocytes
Leukocytes
Monocytes
Platelets
Lymphocytes
Static
Low flow
Standard
High speed
Fold change (S 5 min)
200%
150%
100%
50%
0%
5
120
240
360
Time (min)
B
Plasma Free Haemoglobin
Average pfHb (mg/dL)
15
12
9
6
3
0
0
60
120
180
240
300
360
Time (min)
C
CD45+ LMP
Fold change (S 5 min)
40
30
20
10
0
5
120
240
360
Time (min)

Figure 1.

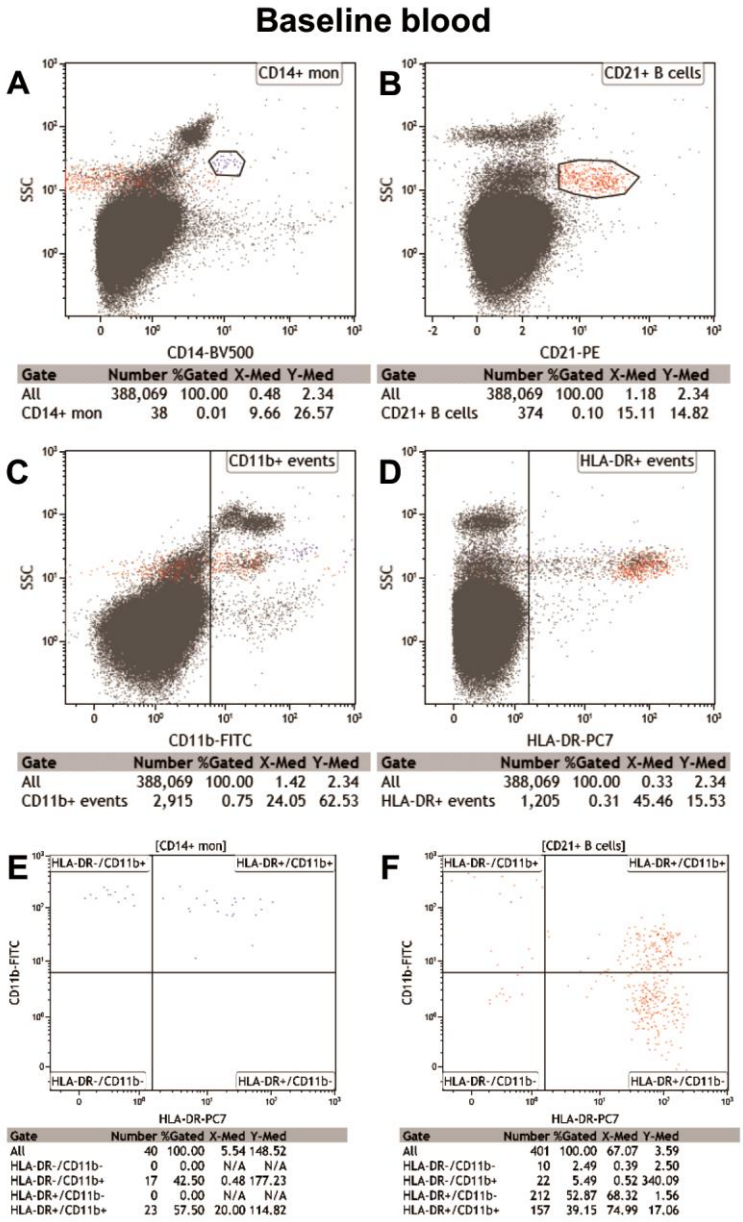
Baseline blood
A
CD14+ mon
SSC
CD14-BV500
Gate Number %Gated X-Med Y-Med
All 388,069 100.00 0.48 2.34
CD14+ mon 38 0.01 9.66 26.57
B
CD21+ B cells
SSC
CD21-PE
Gate Number %Gated X-Med Y-Med
All 388,069 100.00 1.18 2.34
CD21+ B cells 374 0.10 15.11 14.82
C
CD11b+ events
SSC
CD11b-FITC
Gate Number %Gated X-Med Y-Med
All 388,069 100.00 1.42 2.34
CD11b+ events 2,915 0.75 24.05 62.53
D
HLA-DR+ events
SSC
HLA-DR-PC7
Gate Number %Gated X-Med Y-Med
All 388,069 100.00 0.33 2.34
HLA-DR+ events 1,205 0.31 45.46 15.53
E
[CD14+ mon]
HLA-DR-/CD11b+
HLA-DR+/CD11b+
HLA-DR-/CD11b-
HLA-DR+/CD11b-
CD11b-FITC
HLA-DR-PC7
Gate Number %Gated X-Med Y-Med
All 40 100.00 5.54 148.52
HLA-DR-/CD11b- 0 0.00 N/A N/A
HLA-DR-/CD11b+ 17 42.50 0.48 177.23
HLA-DR+/CD11b- 0 0.00 N/A N/A
HLA-DR+/CD11b+ 23 57.50 20.00 114.82
F
[CD21+ B cells]
HLA-DR-/CD11b+
HLA-DR+/CD11b+
HLA-DR-/CD11b-
HLA-DR+/CD11b-
CD11b-FITC
HLA-DR-PC7
Gate Number %Gated X-Med Y-Med
All 401 100.00 67.07 3.59
HLA-DR-/CD11b- 10 2.49 0.39 2.50
HLA-DR-/CD11b+ 22 5.49 0.52 340.09
HLA-DR+/CD11b- 212 52.87 68.32 1.56
HLA-DR+/CD11b+ 157 39.15 74.99 17.06

Figure 2.

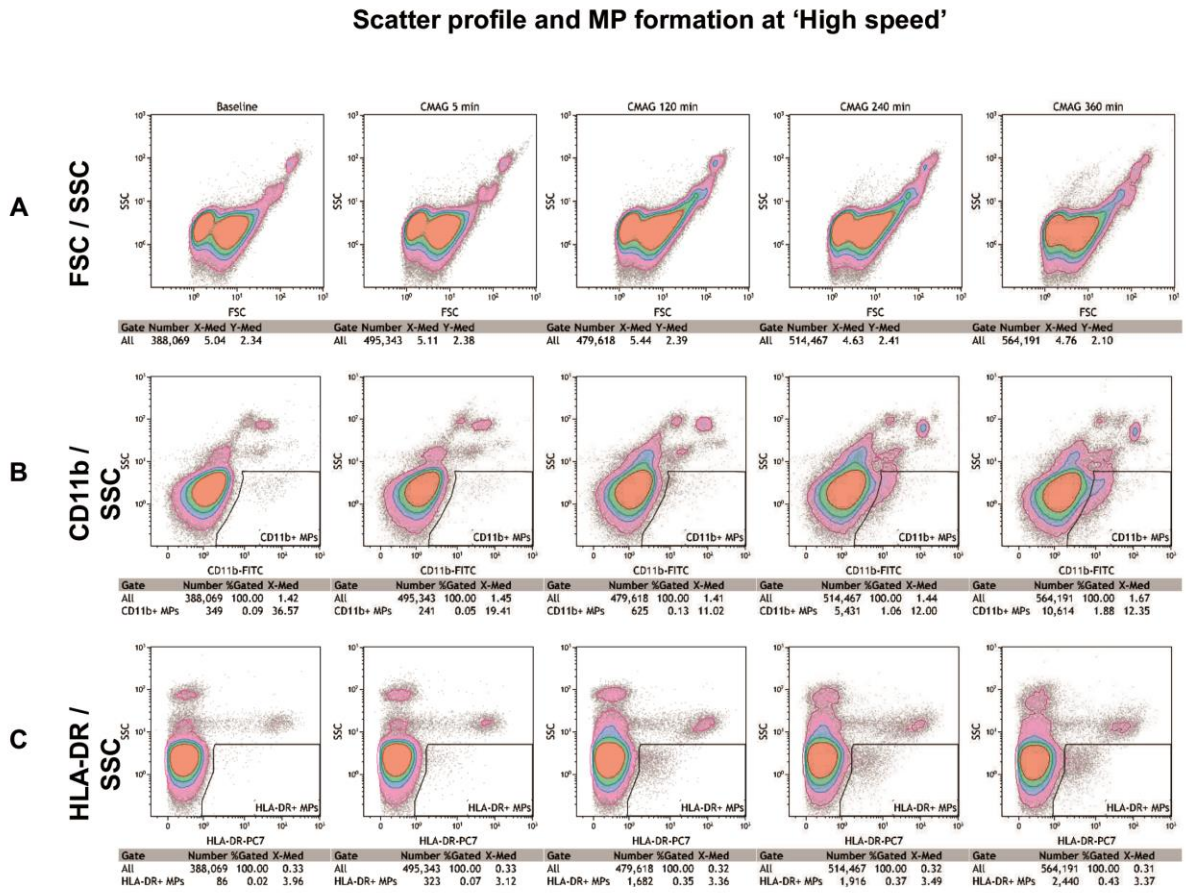
Scatter profile and MP formation at 'High speed'
A
FSC / SSC
B
CD11b / SSC
C
HLA-DR / SSC
Baseline
CMAG 5 min
CMAG 120 min
CMAG 240 min
CMAG 360 min
FSC
SSC
CD11b-FITC
HLA-DR-PC7
CD11b+ MPs
HLA-DR+ MPs
Gate Number X-Med Y-Med
All 388,069 5.04 2.34
All 495,343 5.11 2.38
All 479,618 5.44 2.39
All 514,467 4.63 2.41
All 564,191 4.76 2.10
Gate Number %Gated X-Med
All 388,069 100.00 1.42
CD11b+ MPs 349 0.09 36.57
All 495,343 100.00 1.45
CD11b+ MPs 241 0.05 19.41
All 479,618 100.00 1.41
CD11b+ MPs 625 0.13 11.02
All 514,467 100.00 1.44
CD11b+ MPs 5,431 1.06 12.00
All 564,191 100.00 1.67
CD11b+ MPs 10,614 1.88 12.35
All 388,069 100.00 0.33
HLA-DR+ MPs 86 0.02 3.96
All 495,343 100.00 0.33
HLA-DR+ MPs 323 0.07 3.12
All 479,618 100.00 0.32
HLA-DR+ MPs 1,682 0.35 3.36
All 514,467 100.00 0.32
HLA-DR+ MPs 1,916 0.37 3.49
All 564,191 100.00 0.31
HLA-DR+ MPs 2,440 0.43 3.37

Figure 3.

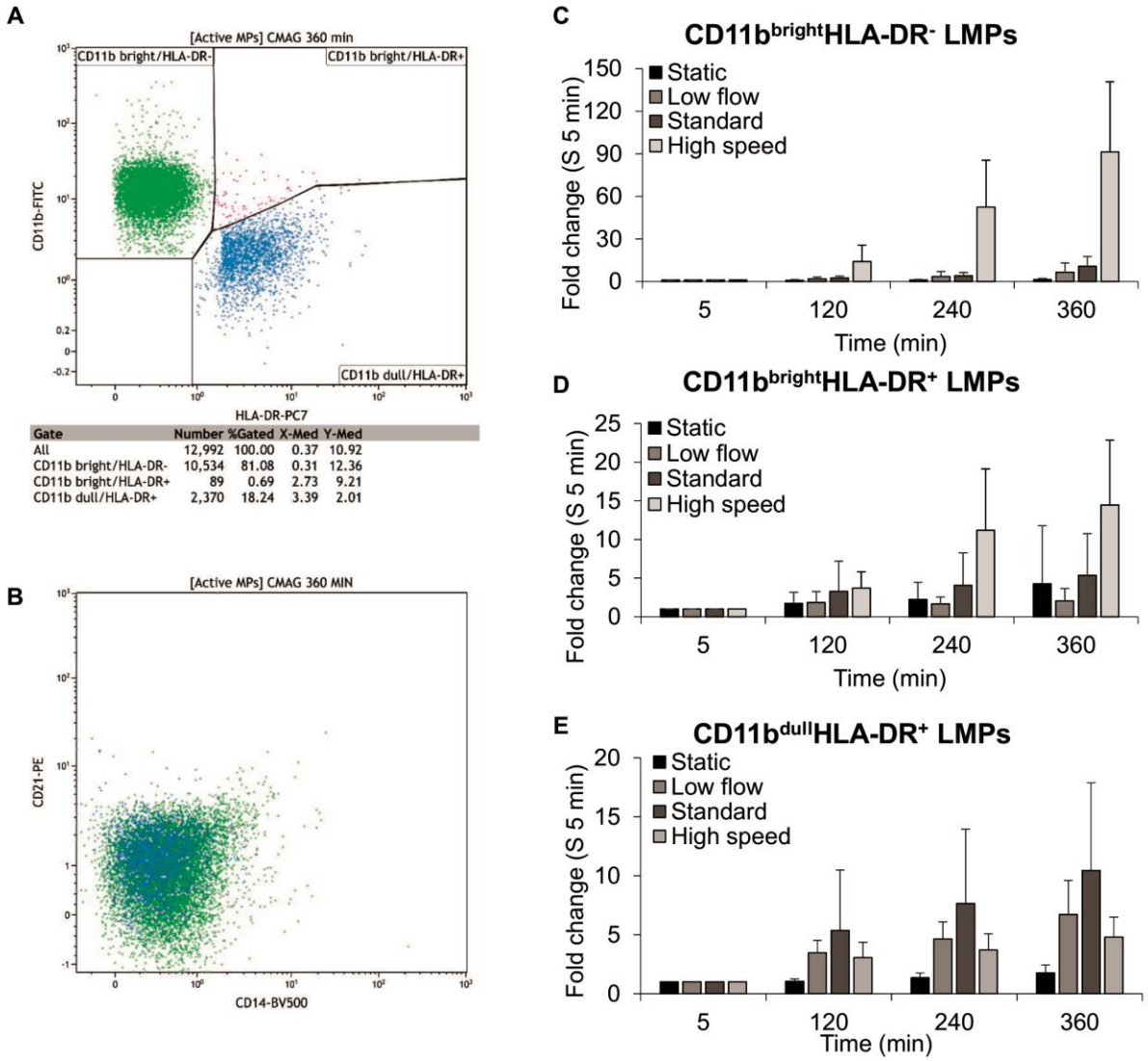
A
[Active MPs] CMAG 360 min
CD11b bright/HLA-DR-
CD11b bright/HLA-DR+
CD11b dull/HLA-DR+
CD11b-FITC
HLA-DR-PC7
Gate Number %Gated X-Med Y-Med
All 12,992 100.00 0.37 10.92
CD11b bright/HLA-DR- 10,534 81.08 0.31 12.36
CD11b bright/HLA-DR+ 89 0.69 2.73 9.21
CD11b dull/HLA-DR+ 2,370 18.24 3.39 2.01
B
[Active MPs] CMAG 360 MIN
CD21-PE
CD14-BV500
C
CD11b^bright HLA-DR- LMPs
Static
Low flow
Standard
High speed
Fold change (S 5 min)
Time (min)
D
CD11b^bright HLA-DR+ LMPs
E
CD11b^dull HLA-DR+ LMPs

Figure 4.

Supplementary Figure Legends

Supplementary figure 1: Gating strategy for the determination of leukocyte microparticles using staurosporine control. Ovine blood (1 ml, baseline sample) treated with 3 μM Staurosporin solution at room temperature for at least 4 h prior to staining with CD45-PE and 7AAD. A. Forward and side scatter plot (log scale) showing the location of leukocytes. B. CD45-PE and side scatter indicating leukocytes as $CD45_+$ events. C. The $CD45_+$ events expressed on a 7AAD and side scatter plot to show healthy, necrotic, and $CD45_+$ microparticles (MPs).

Supplementary figure 2: Fluorescence-minus-one (FMO) and isotype controls. Ovine blood entered into the CentriMag loop and run at 3,300 rpm, 5 L/min (*high speed* condition). Samples were obtained after 4 hours and stained with CD14-BDV500, CD21-PE, CD11b-FITC, and HLA-DR-PE-Cy7 (ALL ABS). In addition, FMO controls were created by omitting one of the antibodies (i.e. CD14-FMO does not contain CD14-BDV500 but the three other antibodies). Isotype controls were created by swapping either CD11b-FITC or HLADR-PE-Cy7 for its isotype control as specified by the manufacturer. Gates were set based on the baseline sample (see Figure 2) and applied to the samples to assess the usefulness of the FMO and isotype controls.

Supplementary figure 3: Comparison of leukocyte microparticle generation over time between static control and CentriMag. Ovine blood was entered into the CentriMag loop and run at 3,300 rpm, 5 L/min (*high speed* condition). A 500 mL bag of ovine blood was left in the +37°C water bath as a static control. Blood samples were removed every 2 hours and stained with CD45-PE and 7AAD.

Supplementary figure 4. Search for CD14+ and CD21+ microparticles. Ovine blood was entered into the CentriMag loop and run at 3,300 rpm, 5 L/min (*high speed* condition). Samples were removed every 2 hours and stained with CD11b-FITC, CD14-BDV500, CD21-PE, and HLA-DR-PE-Cy7. The low side scatter (SSC) region was analysed to see if the number of $CD14_+$ or $CD21_+$ events increased over time.

Supplementary figure 5. Analysis of contaminating platelets. Human blood was entered into the CentriMag loop and run at 3,300 rpm, 5 L/min (*high speed* condition). A sample was removed at 6 hours and stained with CD45-PE, CD41-FITC, and 7AAD. A-C) The $CD45^+$ MPs were gated as previously described. D) The contaminating $CD41^+$ platelet events within the $CD45^+$ MP population were assessed.

Supplementary figure 6. CD45+ LMP method compatibility with Megamix Beads. Megamix beads, 0.5, 0.9 and 3.0 μm in size, were acquired using the standard ovine $CD45^+$ LMP acquisition protocol on the Navios flow cytometer and compared to a previously acquired ovine CD45-PE stained blood sample obtained at 6 hours from the CentriMag when operated at the *high speed* (3,300 rpm, 5 L/min) condition. A-C) The $CD45^+$ LMPs were gated as previously described. D) A 'microparticle' gate was created to include beads ≤ 0.9 μm on a FSC/SSC scatter plot. E) The $CD45^+$ LMPs were displayed on a FSC/SSC scatter plot to assess whether or not they fall within the 'microparticle' gate (92% compatibility).

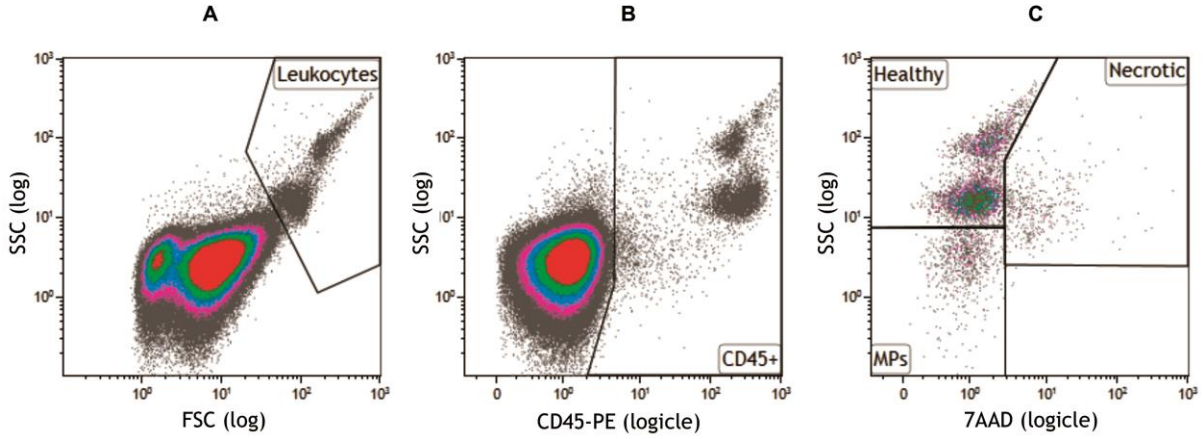

Supplementary Figure 1.

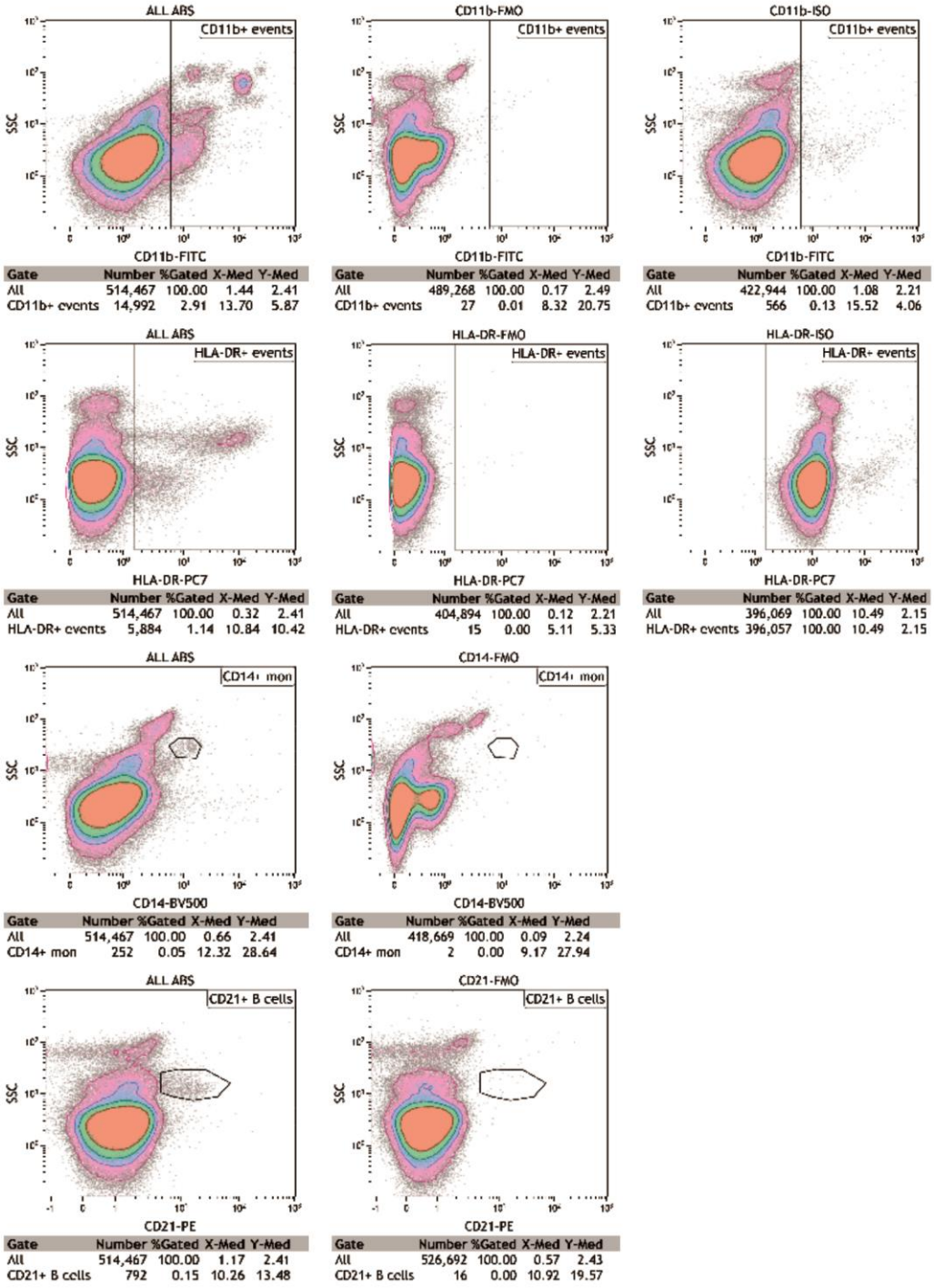

Supplementary Figure 2.

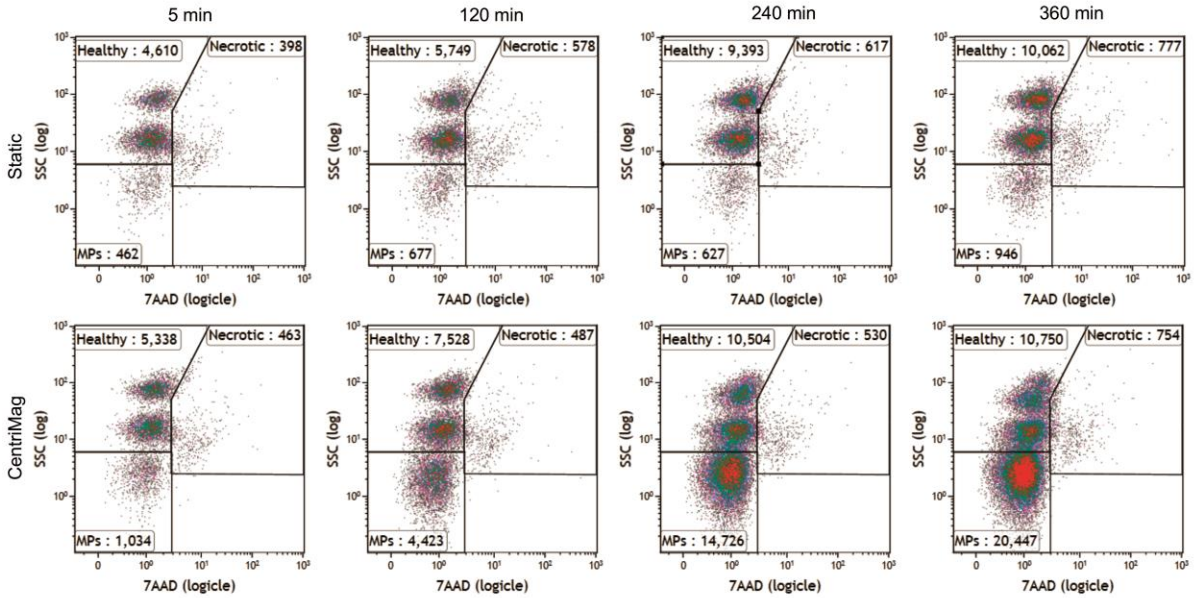

Supplementary Figure 3.

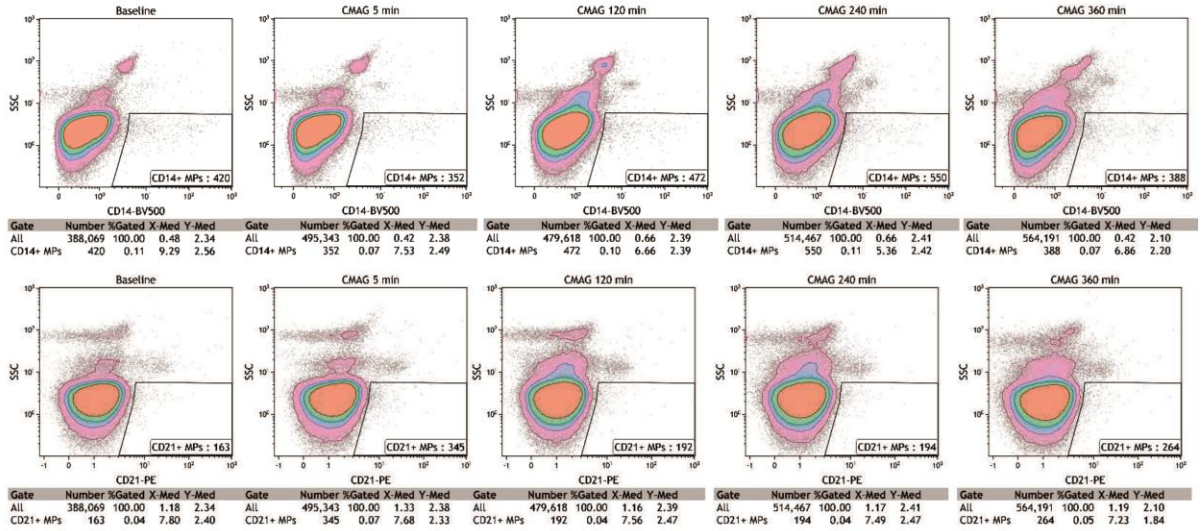

Supplementary Figure 4.

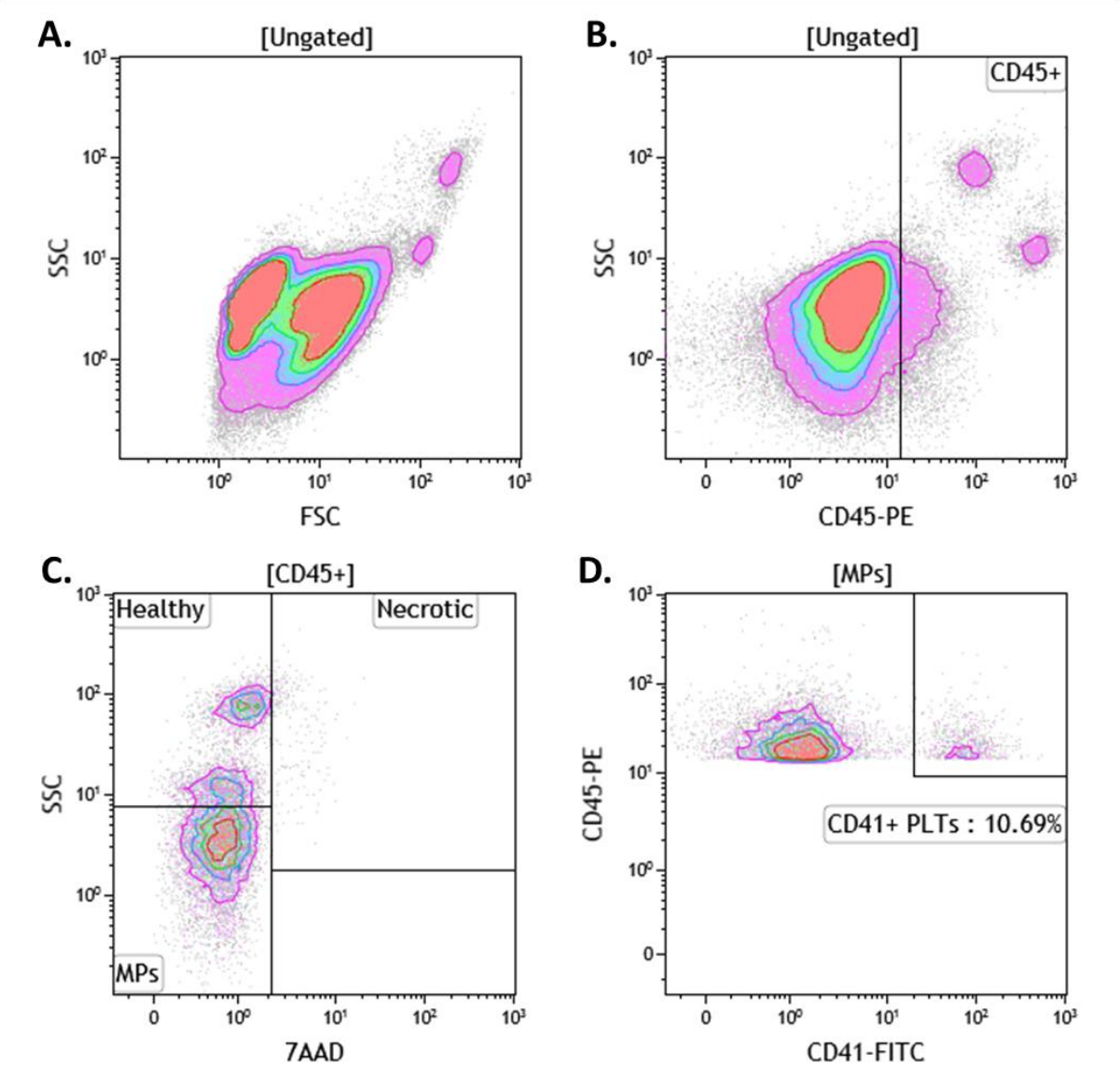

Supplementary figure 5.

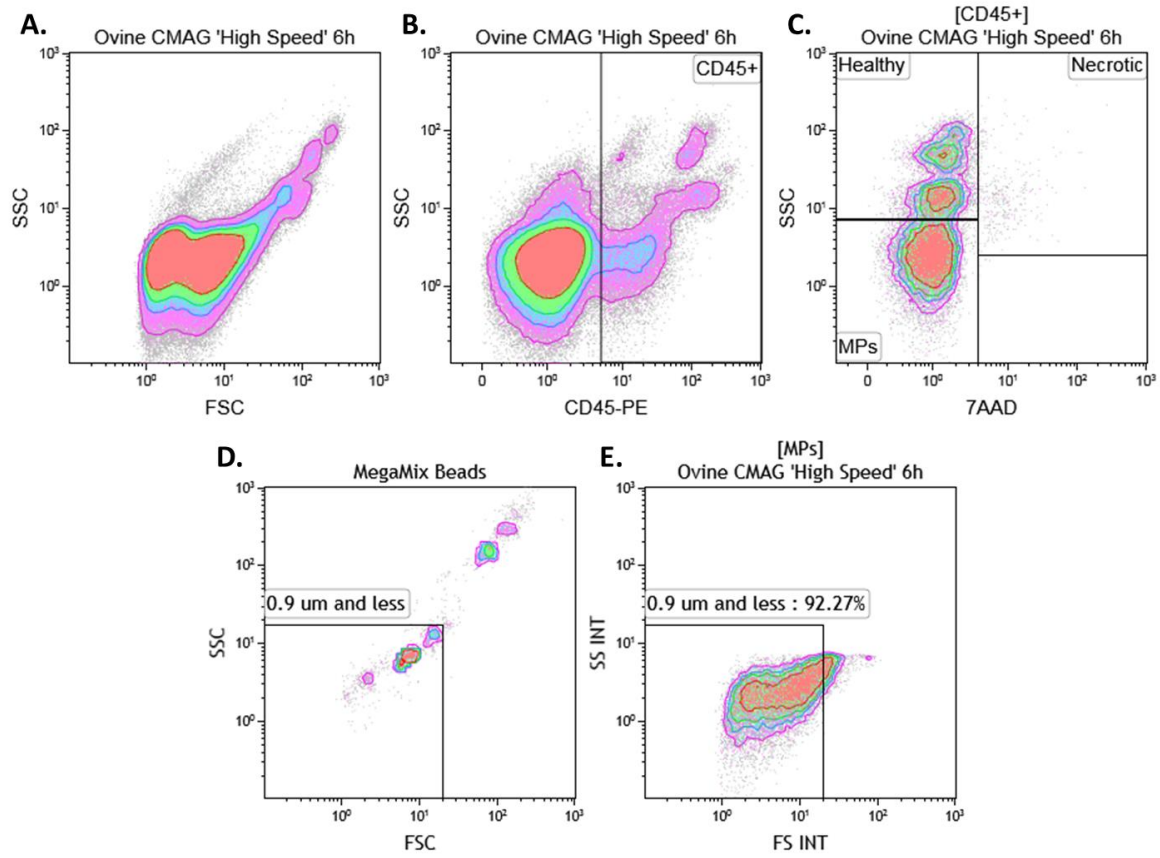

Supplementary figure 6.